THE AMERICAN MINERALOGIST, VOL. 55, MARCH–APRIL, 1970

CRYSTALLOGRAPHIC ASPECTS OF THE CO-CRYSTALLIZATION OF ZEOLITE *L*, OFFRETITE AND ERIONITE

I. S. KERR, J. A. GARD,[1] R. M. BARRER AND ILIANA M. GALABOVA,
Physical Chemistry Laboratories Department of Chemistry, Imperial College of Science and Technology, London, S.W.7.

ABSTRACT

An investigation has been made of zeolite crystallizates in which one or more of offretite, erionite and zeolite *L* are present. Contrary to previous observations X-ray powder patterns can differentiate between offretite and erionite. Where amounts of either crystal are small electron diffraction by single crystallites distinguishes between the species. The offretite and erionite crystals were thereby shown to be faulted in planes normal to the *c*-axis. In characteristic hammer-shaped crystals the shaft tended to be of faulted offretite and the head consisted of zeolite *L*, from which the offretite in the shaft appeared to have grown epitaxially. Zeolite *L* has a predominant flaky habit, whilst offretite and erionite grow as rod-like crystals. The marked tendency to co-crystallization of *L*, offretite and erionite appears to be related to the common structure elements in their aluminosilicate frameworks.

INTRODUCTION

The simultaneous or consecutive growth of natural zeolites seems to occur readily since zeolite deposits usually consist not of one but of several zeolite phases. Specimens resulting from hydrothermal synthesis are also frequently mixtures, sometimes containing intergrowths of more than one species. The present work is a study, mainly by electron diffraction, of the co-crystallization of three distinct but structurally related zeolites offretite, erionite and *L*. Table 1 gives the hexagonal unit cell dimensions and cell contents of the three zeolites. Co-crystallization was thought to be a subject of considerable interest which could lead to a fuller understanding of the mechanism of their hydrothermal crystallization and of the general conditions favouring the appearance of several zeolites in the same crystallizate.

EXPERIMENTAL

The specimens examined in the present work were synthetic samples prepared in these laboratories (Barrer and Galabova, in preparation), and zeolite *L* and zeolite *T* (Breck and Acara, 1965, 1960) grown elsewhere. Zeolite *T* was previously supposed to be erionite. All specimens were in the form of fine powders and were first subjected to X-ray diffraction. Zeolite *L* was frequently found to be contaminated with what appeared to be erionite, and specimens of erionite with zeolite *L*. It

[1] Department of Chemistry, University of Aberdeen, Old Aberdeen, Scotland.

had previously been reported that X-ray powder patterns of offretite and erionite were identical (Hey and Fejer, 1962) and more recently that the two zeolites could readily be distinguished by single-crystal X-ray or electron diffraction, but with less certainty by X-ray powder techniques (Bennett and Gard, 1967). In the present study with synthetic samples it was found however that three fairly strong diffraction arcs occurred only in fully ordered erionite (101, 201 and 211), and could be used for the purpose of distinction (Figure 1 and Table 2). Careful examination of the patterns of natural specimens has confirmed this result (Embrey and Hey, private communication).

As X-ray powder diffraction is not easily able to detect the presence

TABLE 1. THE SPACE GROUPS AND UNIT CELLS WITH THEIR CONTENTS FOR THE THREE ZEOLITES CONSIDERED

Offretite	Erionite	Zeolite *L*
$P\bar{6}m2$	$P6_3/mmc$	$P6/mmm$
$a=13.31$ $c=7.59$ Å	$a=13.26$ $c=15.12$ Å	$a=18.4$ $c=7.5$ Å
$(Ca, Mg, K_2)_{2.5}Al_5$ $Si_{13}O_{36}15H_2O$	$(Ca, Mg, Na_2, K_2)_{4.5}$ $Al_9Si_{27}O_{72}27H_2O$	$K_6Na_3Al_9$ $Si_{27}O_{72}21H_2O$
Bennett and Gard (1967) Sheppard and Gude (1969)	Staples and Gard (1959)	Barrer and Villiger (1969)

of small amounts of impurities, the samples were examined in the electron microscope. All samples showed, in differing proportions, the presence of flakes, rod-like crystals and hammer-shaped crystals as well as conglomerates of these (Fig. 2). The flakes are aggregates *ca.* 4000 Å in diameter, much thicker in the centre than at the edge, and are composed of individual thin plates *ca.* 200–400 Å in diameter (Fig. 3). Carbon replicas published by Breck and Flanigen (1968) have shown that some of the flakes are convex double cones with half angles of *ca.* 50°. Other particles resemble either isolated hammer heads or flakes on edge. Several of the hammer-shaped crystals are shown in Figure 2, from a specimen rich in these crystals. A stereomicrograph at higher magnification (Fig. 3) suggests that the shaft of each hammer is a cylinder joined at one end to a head which is a much thicker aggregate of short prisms. Electron

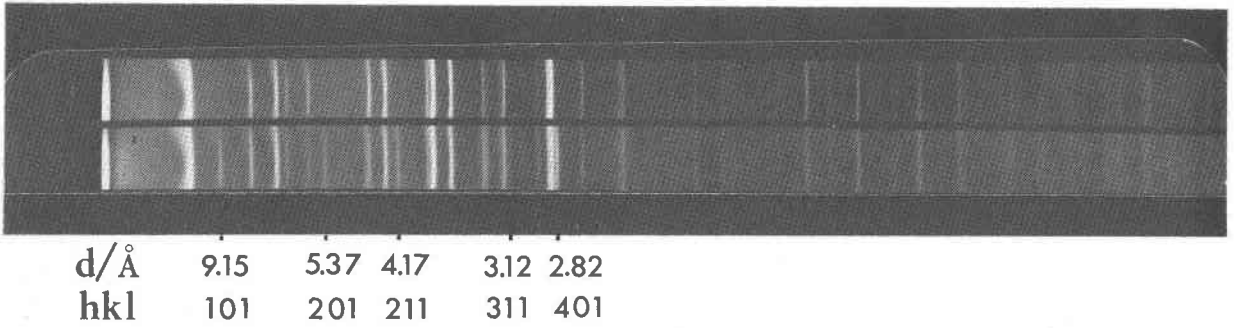

FIG. 1. X-ray powder patterns of (top) synthetic offretite made by Dr. R. Aiello in these laboratories and (bottom) erionite from Jersey Valley, Nevada, U.S.A.

diffraction patterns of the various particles, some with evaporated gold as an internal standard, were interpreted by comparison of measured spot spacings with those calculated from the known unit cells of offretite, erionite and zeolite *L*, given in Table 1. Though it was difficult to obtain the electron diffraction pattern from a single flaky crystal, a few such patterns were recorded (Fig. 4a) and were found to correspond to a crystal of *L* lying on its basal plane. The flake aggregates usually lie on a

TABLE 2. NET PLANE SPACINGS FOR ERIONITE AND OFFRETITE

Erionite		Offretite		Erionite		Offretite	
hkl	*d*/Å	*hkl*	*d*/Å	*hkl*	*d*/Å	*hkl*	*d*/Å
100	11.48	100	11.53	310	3.185	310	3.197
101	*9.145*			204	3.157	202	3.170
002	7.560	001	7.590	*311*	3.117		
110	6.630	110	6.655	303	3.048		
102	6.315	101	6.339	222	3.036	221	3.048
200	5.742	200	5.763	312	2.935	311	2.946
201	*5.368*			105	2.924		
112	4.985	111	5.004	400	2.871	400	2.882
103	4.615			214	2.851	212	2.862
202	4.573	201	4.590	*401*	*2.821*		
210	4.340	210	4.357	313	2.692		
211	*4.172*			304	2.690	302	2.700
300	3.828	300	3.842	402	2.684	401	2.694
203	3.788			205	2.676		
004	3.780	002	3.795	320	2.635	320	2.644
212	3.764	211	3.779	321	2.595		
301	3.711			006	2.520	003	2.530
104	3.591	102	3.605	410	2.506	410	2.515
302	3.415	301	3.428	403	2.495		
220	3.315	220	3.328	224	2.492	222	2.502
213	3.289			322	2.488	321	2.497
114	3.284	112	3.297				

conical face, and give patterns (e.g. Fig. 4b) which represent oblique sections of the reciprocal lattice through an *h*00 row, but weaker *hh*0 spots were also always present. The sharp Laue zones indicate that all the small plates in each aggregate have a common *c*-axial direction. Indices for these patterns suggest a conical half angle of *ca.* 67°. A few patterns were recorded with this *c*-direction parallel to the electron beam; they comprise two hexagonal nets oriented at 30° to one another. Figure 5a shows such a pattern, in which corresponding spots have nearly equal intensities, but in other patterns one net is distinctly stronger than the

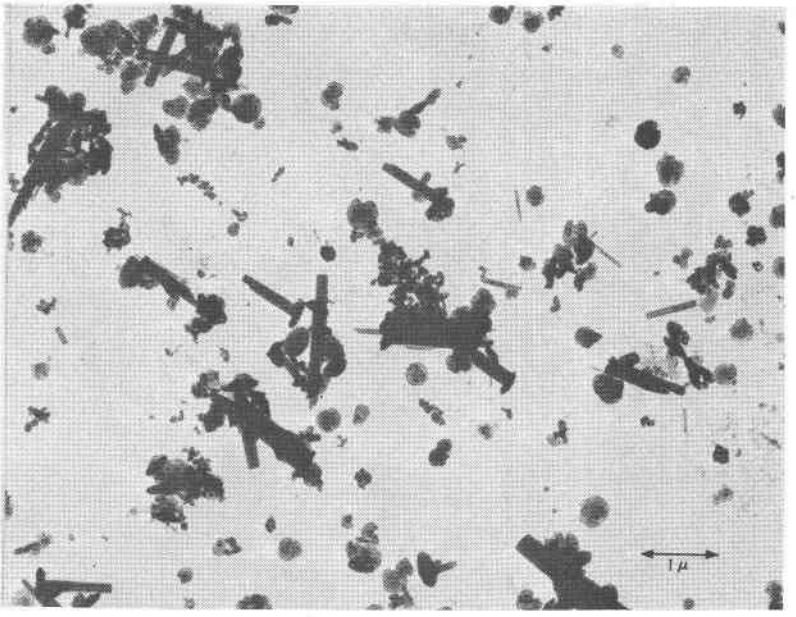

FIG. 2. A general view electron micrograph of the synthetic material showing flaky, rod-like and hammer-shaped crystals.

other. These patterns suggest that the junctions of individual plates are twinned, and the reason for the rotation of 30° may be connected with the presence of nearly planar 12-membered rings. The mean value for a,

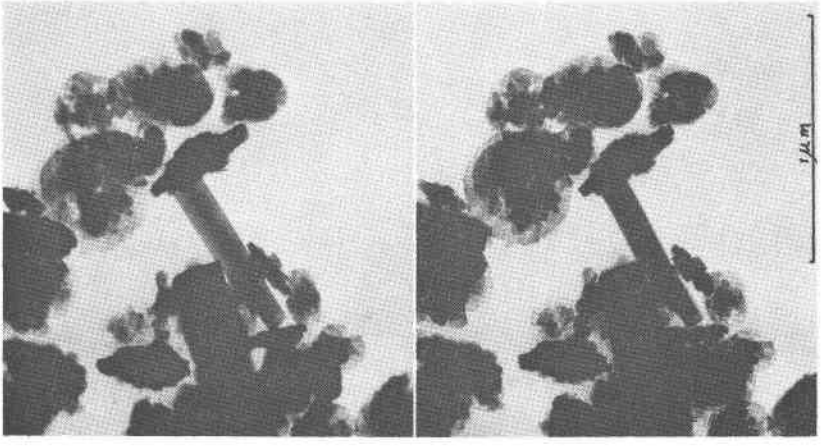

FIG. 3. Stereomicrograph of flaky and hammer-shaped crystals.

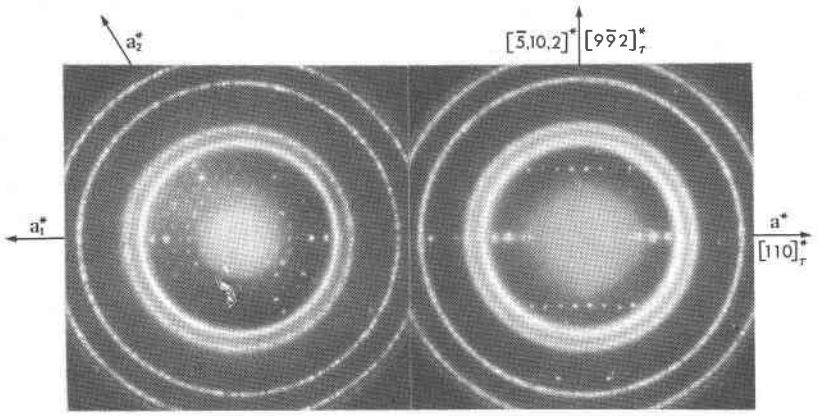

FIG. 4. Electron diffraction patterns from flaky material found to be *L*. (a) beam parallel to *c*-axis, (b) a twinned flake inclined to the beam (suffix τ refers to the twin, although the effect may be due to adhesion). The rings in these patterns (and in Figs. 5a and 7b) are from evaporated gold (d (111) = 2.355 Å etc).

referred to gold, was 18.37 ± 0.05 Å, and rows parallel to a^* could be indexed assuming $c \approx 7.6$ Å in good agreement with the X-ray data; intensities of spots in Figure 5a and other patterns agree qualitatively with the calculated $|F_c|^2$ values of Barrer and Villiger (1969).

Figure 5b shows an electron diffraction pattern from a rod-like crystal which was identified as a faulted erionite. There are streaks running parallel to c, and spots corresponding to l odd are weaker than those for l even. This suggests the occurrence of stacking faults in layers normal to

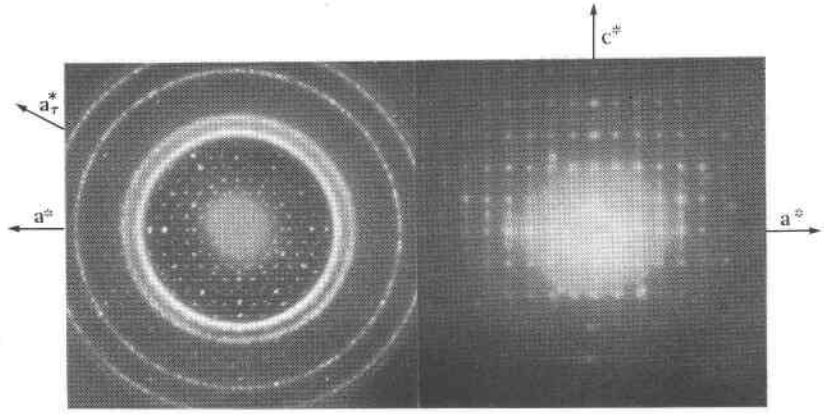

FIG. 5. Electron diffraction patterns from (a) a twinned flake of *L*, normal to the beam showing hexagonal nets at 30°, and (b) a rod of faulted erionite.

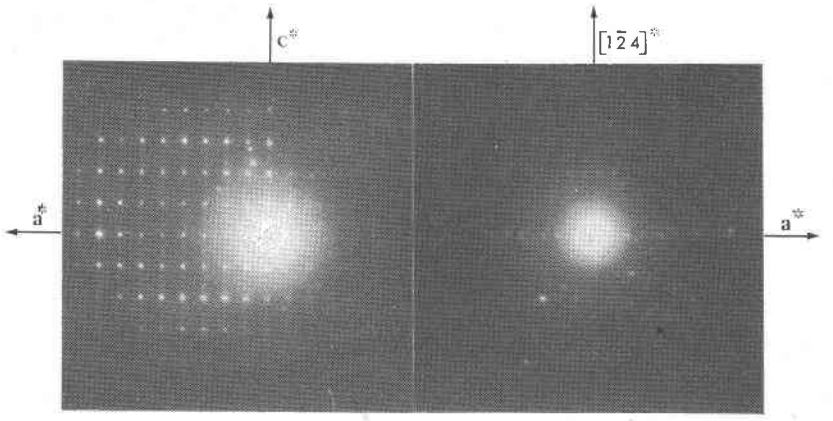

FIG. 6. Electron diffraction patterns from (a) the shaft of a hammer-shaped crystal, resolved as faulted offretite and (b) the head of a hammer, identified as zeolite *L*.

c resulting in small regions of offretite within the crystal[1]. Figure 6a is an electron diffraction pattern obtained from the shaft of a hammer-shaped crystal. The pattern is interpreted as from a faulted offretite with *c* parallel to the shaft. This pattern differs from Figure 5b in that the spots referred to above with *l* odd have now disappeared, but the streaks parallel to *c* still persist. Faults therefore occur in stacking layers normal to *c*. When electron diffraction was directed only at the head of the hammer, the pattern shown in Figure 6b was obtained which corresponds with that of a crystal of zeolite *L* with the *c*-axis in the direction of the shaft. In order to establish the relation between the *a*-axes of the offretite of the shaft and zeolite *L* of the head, electron diffraction patterns were taken to include both parts. The Figures 7a and b show diffraction spots corresponding to the *a**-axes (in a) and the [110]* axes (in b) of offretite and zeolite *L* superimposed on each other (see also Table 3). It is concluded that in the two phases both the *a*- and *c*-axes are parallel.

DISCUSSION

In order to explain the result just described it is necessary to look more closely at the crystal structures. Erionite was the first structure to be determined (Staples and Gard, 1959), while offretite has only recently been distinguished as a different zeolite, although closely related to erionite (Bennett and Gard, 1967). Finally Barrer and Villiger (1969) have determined the structure of zeolite *L*, causing an earlier proposed

[1] This pattern clearly corresponds to an integrowth of erionite and offretite. The exact proportion of each present may be open to debate, but the authors are of the opinion that erionite forms the major part.

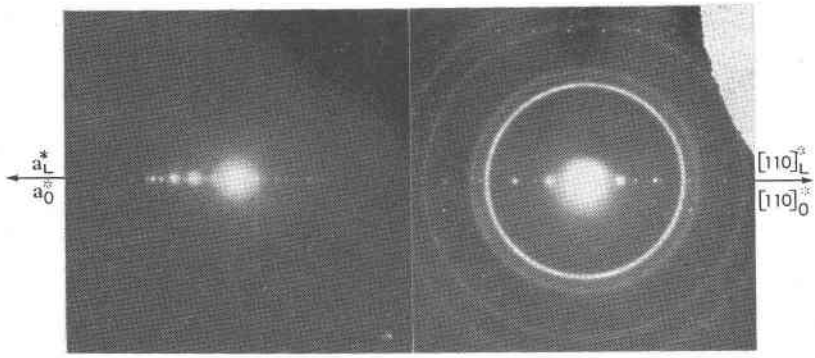

FIG. 7. Electron diffraction patterns of both head and shaft of hammer-shaped crystals a showing a^*-axes of L and offretite superimposed (b) [110]*-axes of L and offretite superimposed. Measurements from these patterns are given in Table 3.

TABLE 3. COMPARISON OF OBSERVED AND CALCULATED RADII FOR FIGURES 7a AND b

	Obs. Rad. Å	Interpretation	Calc. Rad. Å
Fig. 7a			
	0.089	a_0^*	0.087
	0.125	$2a_L^*$	0.126
	0.174	$2a_0^*$	0.174
	0.220	$[220]_L^*$[a]	0.217
	0.261	$3a_0^*$	0.260
	0.313	$5a_L^*$	0.314
	0.348	$4a_0^*$	0.347
	0.375	$6a_L^*$	0.377
	0.435	$5a_0^*$	0.434
Fig. 7b			
	0.153	$[110]_0^*$	0.150
	0.216	$[220]_L^*$	0.217
	0.301	$[220]_0^*$	0.300
	0.326	$[330]_L^*$	0.326
	0.452	$[330]_0^*$	0.451
	0.603	$[440]_0^*$	0.601

[a] Most probably due to 30° twinning of zeolite L.

structure to be discarded (Breck and Flanigen, 1968). All are framework aluminosilicates in which (Si, Al)O^4 tetrahedra join at their apices to form rings of 4, 6, 8 and 12 tetrahedra. Figures 8, 9 and 10 show the three structures projected down the c-axis. Each structure has as building units, 11-hedral cancrinite cages and hexagonal prisms. Identical layers, perpendicular to the c directions exist in erionite and offretite, whilst

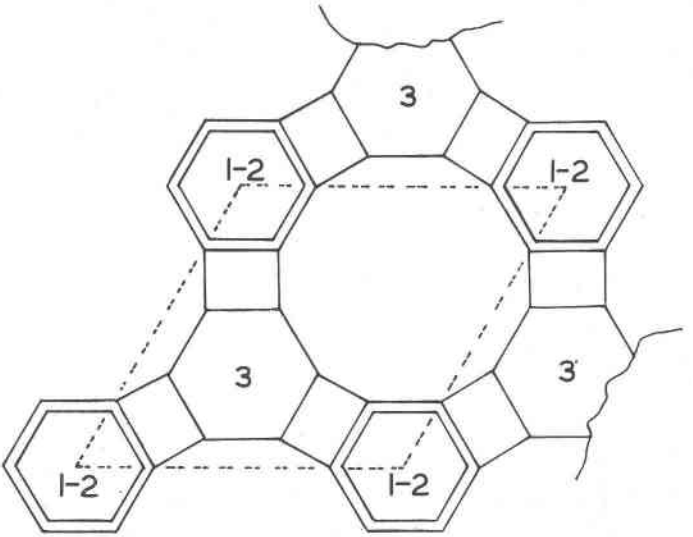

FIG. 8. *c*-projection of offretite. In Figures 8–11, (Si, Al) atoms are represented by the corners, oxygen atoms being ignored. Double six-membered rings are represented by double hexagons, and relative heights of the rings are indicated.

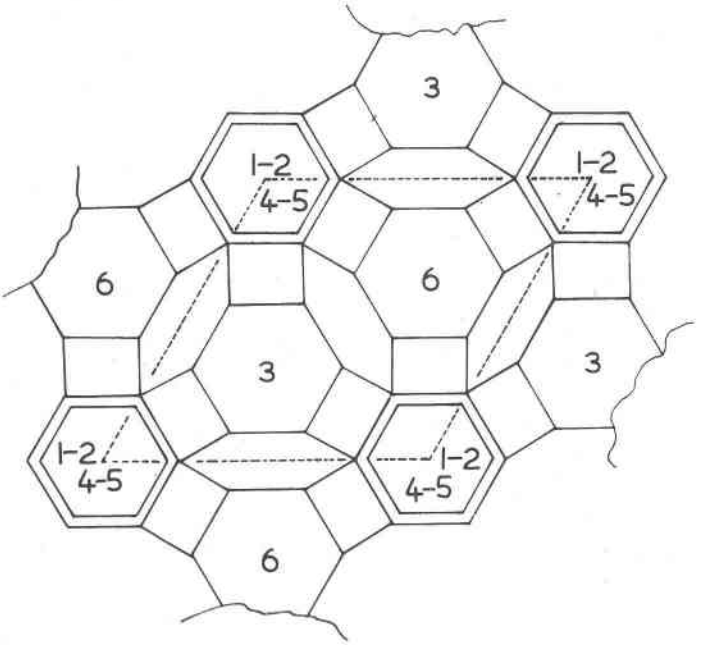

FIG. 9. *c*-projection of erionite.

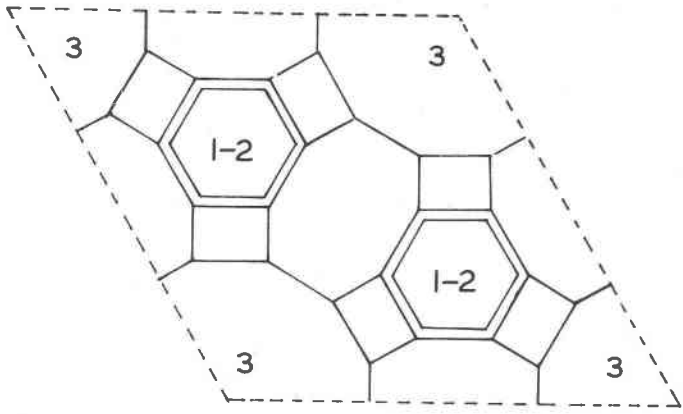

FIG. 10. c-projection of zeolite L.

identical chains parallel to the c direction occur in the L and offretite structures. Figures 8 and 9 show identical layers which occur in erionite and offretite, while Figure 11 shows the chain common to both offretite (centred on $00z$) and zeolite L (positioned at $1/3, 2/3, z$ and $2/3, 1/3, z$). Using the notation in which 6-membered rings centred on the three pos-

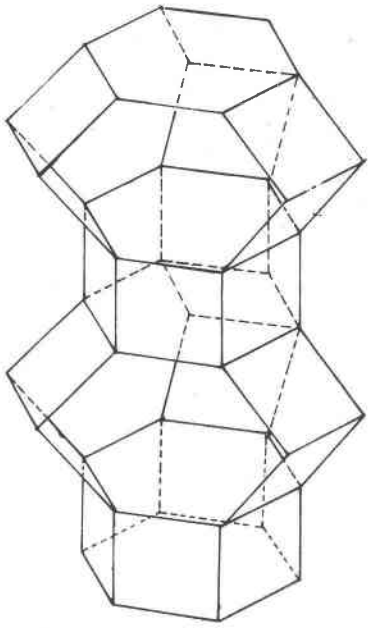

FIG. 11. Chain occurring in both offretite and zeolite L.

sible 6-fold axes in the unit cell are labelled A, B and C, offretite follows an AAB sequence whereas erionite has a longer $AABAAC$ sequence.

The faulting of offretite and erionite can be appreciated when the similarity of the two structures, differing only in stacking sequence, is considered. Faulting will occur where the regular sequence is broken by the occurrence of a random layer, A, B or C. Erionite shows a tendency towards 3-layer repetition and therefore intercalates regions of offretite. Sodalite, which is the only alternative (sequence ABC), is excluded by symmetry considerations. The offretite intercalation is made manifest by the weaker l odd reflections in the pattern (Fig. 5b).

On the other hand faulted offretite shows no tendency for higher periodicity than 3 and so remains essentially an offretite with frequent faults. In general this kind of faulting will entail the presence of A, B and C layers in comparable numbers, with consequent blocking of the main channels and alteration of the molecular sieve behaviour. However, other kinds of faulting can occur in offretite. This faulting may be easily visualised by generating the framework structure of offretite through a

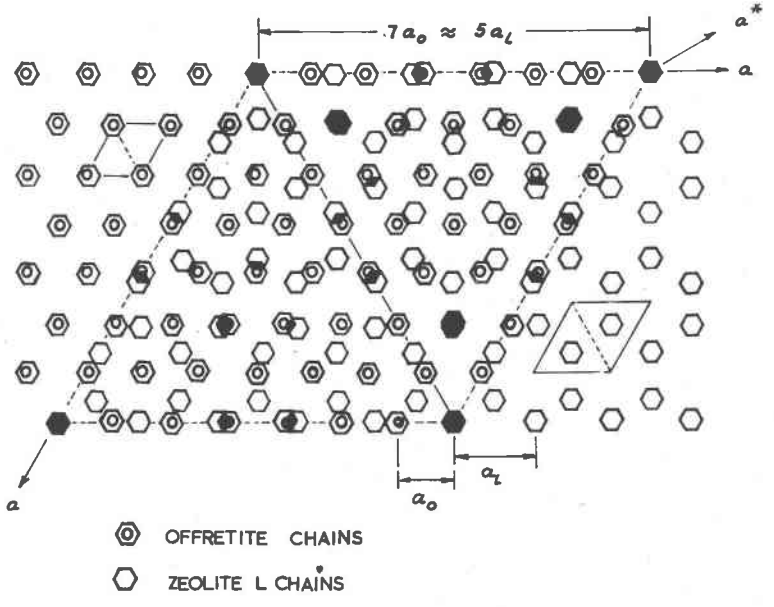

FIG. 12. Projection down the c-axis of identical chains in offretite and zeolite L in the same orientation. Overlapping areas are blackened. Near coincidences occur at intervals along the a-axes of $7a_0 \approx 5a_L$ and at one other chain along each a^*-axis. Out of 49 offretite and 50 zeolite L chains, four almost coincide and could link the head to the shaft in a hammer-shaped crystal.

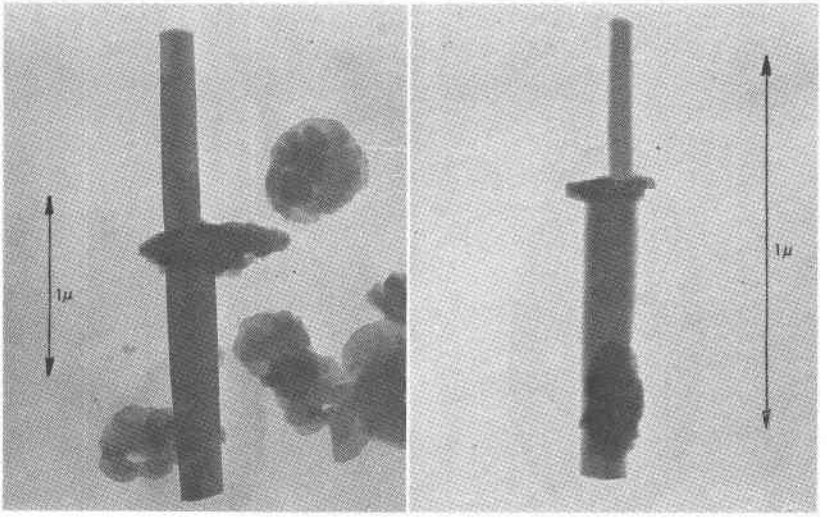

FIG. 13. Electron micrographs of two double headed hammers.

symmetry operation involving chains of 4-membered rings, similar to those occurring in some other zeolites having non-intersecting, parallel main channels (for example zeolite *L*, cancrinite and gmelinite; Barrer and Villiger, 1969). Periodic variations are possible from the ideal offretite chain which can introduce kinds of faulting that do not obstruct the main channels (Barrer and Villiger, 1969, Table 4). These types of faulting cannot be distinguished by electron diffraction from that which blocks the channels, but the molecular sieve behaviour of faulted crystals should serve to differentiate between them.

The hammer-shaped crystals probably owe their peculiar shape to epitaxial growth between a head composed of zeolite *L* and a handle of offretite. Since both structures contain identical chains, similarly orientated with respect to their unit cells, the epitaxy may be explained by some of the chains passing through the interface and effecting a firm union between the two crystals. It would also be necessary for there to be an approximate lattice fit for not one, but a whole array of linking chains. Figure 12 shows a projection down the *c*-axis of the chains in offretite and zeolite *L* upon which certain indicated chains nearly coincide. A coincidence would result in a ratio of $a_L/a_0 = 1.4$, which is close to the experimental value of 1.388 and within the limits set by Wilman (1951). A question which naturally arises here is whether the offretite or the zeolite *L* was present first. However, a careful examination of electron micrographs has revealed several hammers with two shafts, two examples of which are to be found in Figures 13a and b, whereas double-

headed hammers have rarely been observed if at all. These facts seem to indicate that offretite shafts have grown on heads of zeolite *L*.

From the foregoing observations it can be concluded that zeolite *L* grows predominantly in the *a* direction in a flaky habit, whilst offretite and erionite have a preference for growing in the *c* direction in a rod-like habit. The structural causes of the platy habit of zeolite *L*, which is favoured in spite of the presence of the chains accounting for the fibrous, acicular or prismatic habits of offretite and erionite, are not known. The appearance of hammer-shaped crystals in a given sample is an indication of the presence of both offretite and zeolite *L* and can be used as such when the X-ray powder method fails to show their presence. Hammer-shaped crystals have been encountered previously but not identified (Breck and Flanigen, 1968). It is always advisable to examine specimens of offretite and erionite by electron diffraction to detect whether faulting occurs. This is particularly important when samples are intended as sorbents because, for example, the presence of a faulted offretite in a specimen of erionite could alter the sorbent properties, while the presence of an unfaulted offretite could produce an even more marked effect (Barrer and Galabova, in preparation). X-ray powder diffraction fails to distinguish between offretite and structural intergrowths such as zeolite *T* in which there is a fairly high proportion of erionite stacking.

The simultaneous growth of the three zeolites, all of which possess the same building units (cancrinite cages and hexagonal prisms), suggest that such units may be created in solution as precursors to nucleation of crystal growth. Such units may well originate from chains and rings of SiO_4^{4-} and AlO_4^{5-} tetrahedra, surrounding a cation in solution. Condensation-polymerization of polygonal and polyhedral ions, as discussed before (Barrer, 1967), may then result in formation of stable nuclei. This mechanism is supported by the fact that cations are included within these units in the final structures (Barrer and Villiger, 1969; Gard, Bennett and Ingram, in preparation).

ACKNOWLEDGMENT

One of us (I.M.G.) wishes to acknowledge with thanks the award of a grant from W. R. Grace and Co., which enabled her to take part in this work.

REFERENCES

BARRER, R. M. (1967) Mineral synthesis by the hydrothermal technique, *Chem. Britain*, **3**, 380–394.

———, AND H. VILLIGER (1969) The crystal structure of the synthetic zeolite *L*; *Z. Kristallogr.* **128**, 352–370.

BENNETT, J. M. AND J. A. GARD (1967) Non-identity of the zeolites erionite and offretite. *Nature* **214**, 1005–1006.

BRECK, D. W. AND N. A. ACARA, (1962) Synthetic crystalline zeolite *L*, *Brit. Pat.* 909,264.

——— AND ——— (1960) Crystalline zeolite *T*, *U.S. Pat.* **2,950,952**.

——— AND E. M. FLANIGEN (1968) Synthesis and properties of Union Carbide zeolites *L*, *X* and *Y*. *Molecular Sieves. Conf. Rep. Soc. Chem. Ind., London*, pp. 47–60.

HEY, M. H. AND E. E. FEJER, (1962) The identity of erionite and offretite. *Mineral. Mag.* **33**, 66–67.

SHEPPARD, R. A. AND A. J. GUDE (1969) Chemical composition and physical properties of the related zeolite offretite and erionite. *Amer. Mineral.* **54**, 875–886.

STAPLES, L. W. AND J. A. GARD, (1959) The fibrous zeolite erionite; its occurrence, unit cell, and structure. *Mineral. Mag.* **32**, 261–281.

WILMAN, H. (1951) The slip, twinning, cohesion, growth and boundaries of crystals. *Proc. Phys. Soc., London*, **A64**, 329–350.

Manuscript received, October 5, 1969; accepted for publication, November 2, 1969.